trophs increased with time and eventually reached 25% of the dominant population after 400 days (Fig. 3). In mice inoculated with *mutS*$^+$ ancestors, the proportion of auxotrophs also increased, but only reached a maximum of 5%. Ninety percent of these auxotroph bacteria could be attributed to mutator subpopulations that had spontaneously emerged in some mice (Fig. 3). It appears that during intestinal colonization mutator bacteria lose robustness because of the accumulation of neutral mutations (*20*) that become deleterious in secondary environments. This may explain why mutator bacteria do not represent a larger fraction of natural isolates (*1*, *2*).

To assess the relative importance of mutator-associated costs and benefits when bacteria experience both primary and secondary environments, we inoculated two mice: one with wild-type, the other one with mutator bacteria. Both were placed in the same cage with a third, initially germ-free, mouse. By summing the populations of mutator and wild-type strains subsequently colonizing the three mice (metapopulation), we monitored the combined effects on population sizes of competition in the gut and migration of bacteria between mice. In contrast to 1:1 competition, the competitive advantage of the mutator allele was not detectable in these metapopulations (Fig. 2D). When the same metapopulation experiment was done with mice inoculated with populations previously grown for 400 days in separate mice, the mutator metapopulation remained lower than the wild type (Fig. 2D), showing the prevailing effect of the costs associated with a mutator allele once the adaptive mutations have been acquired.

The mouse model showed that the advantage of mutator bacteria when colonizing new host is due to their capacity to generate adaptive mutations rapidly, allowing them to exploit the ecosystem resources more quickly than wild-type bacteria. This advantage is reduced to little or nothing once adaptation is achieved. Moreover, if the mutation rate is not reduced [as observed in some subpopulations (Fig. 1A)], it leads progressively to loss of functions that are dispensable in the current environment but compromise the long-term survival of mutator clones. Our experiments also showed that bacterial migration between hosts is a potent factor in reducing the benefits of enhanced mutation rate and should be taken into consideration for understanding the dynamics of mutator bacteria in natural populations. The heterogeneity of natural environments might be expected to favor variability in mutation rate, as we observed in some bacterial populations colonizing mice (Fig. 1A). This in vivo study shows that important variations of the mutation rate can happen within weeks. These results may account for the observation that some natural bacterial isolates, such as those of *Pseudomonas aeruginosa* found in the lungs of cystic fibrosis patients, have a strong mutator phenotype. It may also inspire studies on emerging pathogenicity and drug resistance in microorganisms (*2*, *4*, *21*, *22*), as well as assisting studies on the somatic evolution of malignant mutator tumor cells (*23*).

References and Notes

1. I. Matic *et al.*, *Science* **277**, 1833 (1997).
2. J. E. LeClerc, B. Li, W. L. Payne, T. A. Cebula, *Science* **274**, 1208 (1996).
3. M. D. Gross, E. C. Siegel, *Mutat. Res.* **91**, 107 (1981).
4. A. Oliver, R. Cantón, P. Campo, F. Baquero, J. Blázquez, *Science* **288**, 1251 (2000).
5. L. Chao, E. C. Cox, *Evolution* **37**, 125 (1983).
6. E. F. Mao, L. Lane, J. Lee, J. H. Miller, *J. Bacteriol.* **179**, 417 (1997).
7. P. D. Sniegowski, P. J. Gerrish, R. E. Lenski, *Nature* **387**, 703 (1997).
8. W. Tröbner, R. Piechocki, *Mol. Gen. Genet.* **198**, 175 (1984).
9. F. Taddei *et al.*, *Nature* **387**, 700 (1997).
10. O. Tenaillon, B. Toupance, H. Le Nagard, F. Taddei, B. Godelle, *Genetics* **152**, 485 (1999).
11. M. Radman, I. Matic, J. A. Halliday, F. Taddei, *Philos. Trans. R. Soc. Lond. B* **347**, 97 (1995).
12. B. Picard *et al.*, *Infect. Immun.* **69**, 9 (2001).
13. Supplemental text describing detailed methods and results, Web figures 1 through 4, and Web table 1 are available at *Science* Online at www.sciencemag.org/cgi/content/full/291/5513/2606/DC1.
14. Given that rifampicin-resistant mutants are not selected for in the mouse gut, their frequency is an indicator of the overall population mutation rate (*13*).
15. The mutation rate of a clone from mouse m2 (Fig. 1) transformed with a plasmid carrying the *mutH* wild-type allele was reduced to its wild-type ancestor level. The mutation rate of a clone from mouse m1 (Fig. 1) was reduced to its wild-type ancestor level when transformed with a plasmid carrying *mutS* or *mutH* wild-type alleles. Results of the complementation are available at (*13*).
16. Switching the antibiotic resistance markers had no effect on competition. Detailed description of the strain construction is available at (*13*).
17. J. Arjan *et al.*, *Science* **283**, 404 (1999).
18. The fixation of neutral or deleterious mutations in populations with a high mutation rate undergoing strong bottlenecks is known as Muller's ratchet [H. Muller, *Mutat. Res.* **1**, 2 (1964); P. Funchain, *et al.*, *Genetics* **154**, 959 (2000)]. To model our experimental conditions, the accumulation of neutral mutations in large populations subjected to directional selection was simulated on the basis of the model published by Tenaillon *et al.* (*10*). Even if the increase in the frequency of selective sweeps in mutator populations depended on the strength of selection, neutral mutations always accumulated 100-fold faster than in nonmutator populations (data not shown).
19. D. L. Hartl, D. E. Dykhuizen, *Annu. Rev. Genet.* **18**, 31 (1984).
20. Different types of auxotrophs were isolated both between and within mice, thus suggesting that these mutations were not adaptive. See (*13*).
21. C. Bucci *et al.*, *Mol. Cell* **3**, 435 (1999).
22. M. A. Wainberg *et al.*, *Science* **271**, 1282 (1996).
23. L. A. Loeb, *Adv. Cancer Res.* **72**, 25 (1998).

24. We are grateful to J. P. Coutanceau, A. M. Cirinesi, and C. Dohet for their technical help; F. Marcille for her constructive discussion; and D. Brégeon, L. Le Chat, V. Colot, M. S. Fox, E. C. Friedberg, B. Godelle, A. Gomez, E. Stewart, and M. Vulic for comments on the manuscript. Funded by the Ligue contre le cancer, the Association de la Recherche contre le Cancer, the Programme Environnement et Santé (MATE), the Fondation pour la recherche Médicale, and the Programme de Recherche Fondamentale en Microbiologie et Maladies Infectieuses et Parasitaires (MENRT).

9 October 2000; accepted 2 February 2001

Virus-Assisted Mapping of Neural Inputs to a Feeding Center in the Hypothalamus

Jeff DeFalco,[1] Mark Tomishima,[2] Hongyan Liu,[1] Connie Zhao,[3] XiaoLi Cai,[1] Jamey D. Marth,[4,5] Lynn Enquist,[2] Jeffrey M. Friedman[1,3]*

We report the development of a pseudorabies virus that can be used for retrograde tracing from selected neurons. This virus encodes a green fluorescent protein marker and replicates only in neurons that express the Cre recombinase and in neurons in synaptic contact with the originally infected cells. The virus was injected into the arcuate nucleus of mice that express Cre only in those neurons that express neuropeptide Y or the leptin receptor. Sectioning of the brains revealed that these neurons receive inputs from neurons in other regions of the hypothalamus, as well as the amygdala, cortex, and other brain regions. These data suggest that higher cortical centers modulate leptin signaling in the hypothalamus. This method of neural tracing may prove useful in studies of other complex neural circuits.

The decision to initiate feeding is dependent on a variety of motivational, metabolic, and hormonal factors including the plasma level of leptin (*1*, *2*). Leptin is an adipocyte-derived hormone whose effects on food intake are mediated through distinct classes of neurons that express the leptin receptor. These neurons are distributed among several hypothalamic nuclei including the arcuate nucleus (ARC) and the ventromedial (VMH), lateral (LH), and dorsomedial (DMH) nuclei (*3*). Although neurons in these nuclei are

known to receive inputs from other brain regions, the precise nature of these inputs has not been established. Identification of such neural inputs requires that one be able to trace neural connections across one or more synapses.

Pseudorabies virus (PRV) has been used previously to trace neural circuits across multiple synapses (*4*, *5*). After injection of PRV into a number of peripheral sites, including the heart, gastrointestinal tract, and liver, viral antigens can be detected in precisely those brain regions known to innervate these organs. PRV has also been used to trace polysynaptic circuits after direct injection into the central nervous system (CNS) (*6*). However, because the virus infected many different neurons, no information could be deduced regarding inputs to specific classes of neurons, for example, those expressing a particular neurotransmitter, neuropeptide, or receptor. Here, we report the development of a recombinant PRV that is dependent on a Cre-mediated recombination event for replication and for expression of green fluorescent protein (GFP). This virus was used to map CNS inputs to hypothalamic neurons that play a role in regulating food intake.

The Bartha strain of PRV is an attenuated live vaccine strain that is propagated primarily in a retrograde fashion (opposite to the direction of impulse transmission) along chains of synaptically connected neurons. We constructed a PRV-Bartha strain that was conditional both for replication (in nonmi-

[1]Howard Hughes Medical Institute, The Rockefeller University, New York, NY 10021, USA. [2]Department of Molecular Biology, Princeton University, Princeton, NJ 08544, USA. [3]Laboratory of Molecular Genetics, The Rockefeller University, New York, NY 10021, USA. [4]Howard Hughes Medical Institute, University of California, San Diego, CA 92093, USA. [5]Department of Cellular and Molecular Medicine, University of California, San Diego, CA 92093, USA.

*To whom correspondence should be addressed. E-mail: friedj@mail.rockefeller.edu

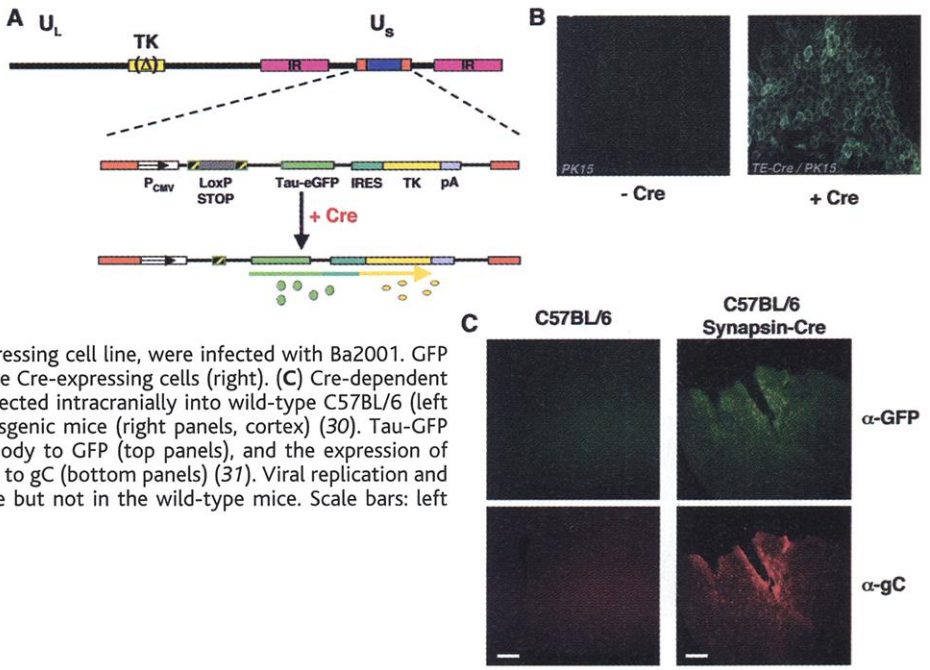

Fig. 1. Structure and expression properties of PRV strain Ba2001. (**A**) A recombinant PRV that is dependent on a Cre-mediated recombination event for expression of TK and GFP was created. The parent virus, PRV-Bartha Blue (BaBlu) carries a deletion in the *tk* gene. The elements of the targeting construct pG2LTHTK are shown below the region of recombination into the *gG* region of Bartha Blue. Flanking *gG* sequence is indicated by the red stippled boxes; *lacZ* open reading framed is indicated by the blue stippled box. Successful recombination of the targeting cassette replaces *lacZ*, resulting in a white plaque. (**B**) Conditional expression of Tau-GFP in tissue culture cells. PK15 cells or TE-Cre cells, a Cre-expressing cell line, were infected with Ba2001. GFP expression was observed only after infection of the Cre-expressing cells (right). (**C**) Cre-dependent GFP expression in Syn1-Cre mice. Ba2001 was injected intracranially into wild-type C57BL/6 (left panels, hypothalamus) or C57BL/6 Syn1-Cre transgenic mice (right panels, cortex) (*30*). Tau-GFP was detected by immunofluorescence from antibody to GFP (top panels), and the expression of viral late protein gC was detected using antibodies to gC (bottom panels) (*31*). Viral replication and expression of GFP were observed in the Syn1-Cre but not in the wild-type mice. Scale bars: left panel, 200 μm; right panel, 100 μm.

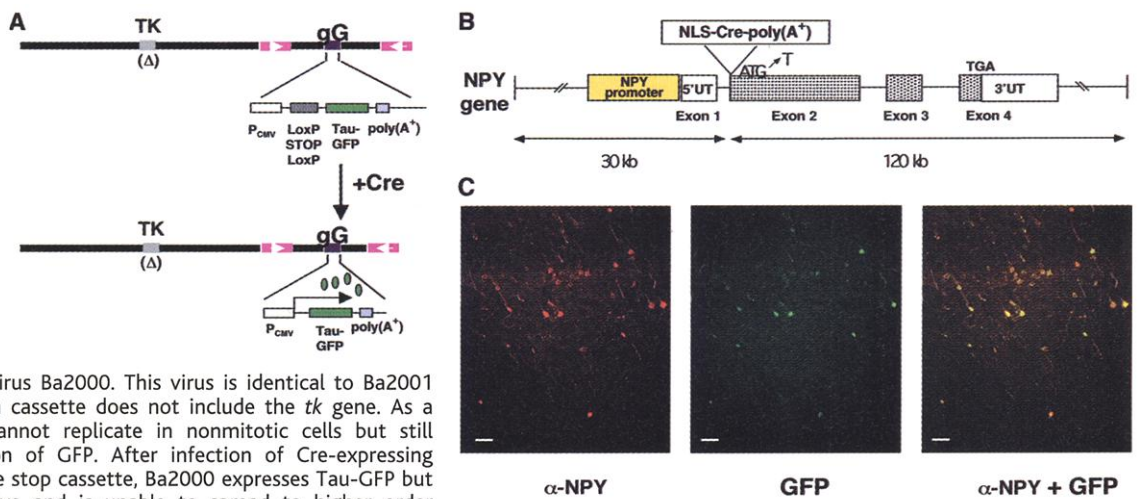

Fig. 2. Specificity of Cre recombination in NPY-expressing cells in vivo. The in vivo requirement of *Cre* for excision of the *Lox*-stop cassette was tested in mice that express Cre only in NPY-expressing neurons. A *tk*$^-$ virus that was conditional only for GFP was used to infect a transgenic mouse that carried a 150-kb BAC in which *Cre* had replaced the *Npy* coding region. (**A**) Replication-defective virus Ba2000. This virus is identical to Ba2001 except that the expression cassette does not include the *tk* gene. As a consequence, this virus cannot replicate in nonmitotic cells but still requires Cre for expression of GFP. After infection of Cre-expressing neurons and deletion of the stop cassette, Ba2000 expresses Tau-GFP but remains replication-defective and is unable to spread to higher order neurons. This strategy allows first-order neurons to be visualized exclusively. (**B**) A BAC transgenic mouse was developed in which the *Npy* gene was replaced by *Cre*. A nuclear localization sequence–*Cre* open reading frame (NLS-*Cre*)–polyadenylation sequence [poly(A$^+$)] was inserted 5′ to the ATG in the first exon of the *Npy* gene. This BAC includes 30 kb of 5′ upstream and 120 kb of downstream sequence and leads to expression of *Cre* in NPY neurons. (**C**) GFP expression is limited to NPY-expressing neurons. Ba2000 was injected into the somatosensory 2 cortex of *Npy-Cre* transgenic mice. Sections were stained for NPY or GFP. An overlay of the NPY and GFP immunofluorescence images (right panel) indicates that GFP expression is only observed in neurons that express NPY (yellow cells). Scale bars, 100 μm.

totic cells) and for expression of the Tau-GFP marker (Fig. 1A). We first introduced a deletion into the endogenous thymidine kinase (*tk*) gene of a recombinant PRV that already carried an insertion of the *lacZ* gene in the *gG* locus (TK-BaBlu) (*7*). The *gG* gene is dispensable for replication (*8*). We next created a bicistronic expression cassette in which the cytomegalovirus (CMV) immediate early promoter was cloned upstream of a *Tau-GFP* fusion gene followed by an internal ribosome entry site (IRES) immediately 5′ to the herpes simplex virus *tk* gene (*9*). A *Lox*-Stop-*Lox* cassette was inserted between the CMV promoter and the start of the *Tau-GFP* open reading frame. This stop cassette, which is composed of two *LoxP* elements flanking an SV40 polyadenylation signal and 5′ splice donor site, prevents expression of downstream sequences unless it is removed by Cre-mediated recombination (*10*). Thus, expression of both *tk* and *GFP* is conditional and requires a Cre-mediated recombination event. This construct was then used to replace the *lacZ* insert in the TK-BaBlu virus by homologous recombination. The recombinant virus, which we named Ba2001, was initially identified by the loss of β-galactosidase (β-gal) activity and further characterized by Southern blot analysis (*11*).

Because TK is required for viral DNA synthesis in neurons, Ba2001 would not be expected to replicate in neurons that do not express Cre recombinase (*12*). Infection of a neuron that expresses Cre would be expected to lead to the removal of the stop signals thereby rendering the virus capable of replicating in other neurons in synaptic contact with the original neuron. These infected neurons should also express GFP. The removal of the stop signals is permanent, allowing the subsequent retrograde infection and labeling of any afferent neurons whether or not they express Cre. Conditional expression of GFP in Ba2001 was confirmed by infecting untransfected PK15 and Cre-expressing TE-Cre fibroblasts (*13*). GFP fluorescence was never observed in Ba2001-infected cells that did not express Cre but was readily detectable in the infected Cre-expressing cells (Fig. 1B).

Viral replication and GFP expression in vivo were also dependent on Cre-mediated recombination (Fig. 1C). Ba2001 was injected intracranially into wild-type C57BL/6 mice and C57BL/6 transgenic Syn1-Cre mice. Mice from the latter strain express Cre in all neurons because the *Cre* gene is under the control of a 4.4-kb neuron-specific rat synapsin promoter (*14*). Five days after infection, significant GFP fluorescence was observed in the cortex of Cre-expressing mice but not in the wild-type mice (Fig. 1C). The GFP-expressing neurons also stained for the gC protein, a late viral protein, expressed only after viral DNA replication (*15*).

To demonstrate that the stop cassette had been excised in vivo, we injected 2.4×10^6 plaque forming units (PFUs) of Ba2001 into the striatum of wild-type and Syn1-Cre mice and killed the animals 7 days later (*16*). Lysates were prepared from the contralateral striatum of each animal and used to infect PK15 cells in culture. Individual virus plaques were counted and scored for GFP fluorescence. We recovered 75 fluorescent plaques out of a total of 76 plaques per microliter from the lysates of infected Syn1-Cre mice and no fluorescent plaques (0/7) from infected wild-type mice. This indicates that the virus had undergone Cre-mediated recombination in vivo. Southern blots confirmed that the Lox cassette had been removed in the fluorescent viruses (*17*).

We next used Ba2001 to trace the connections from neurons in which Cre expression was restricted to neurons that express the *neuropeptide Y* (*Npy*) gene. NPY is a 36–amino acid peptide that increases food intake and body weight after intracranial or intrahypothalamic injections (*18*, *19*). NPY is abundantly expressed in neurons in a large number of brain regions including the cortex, medulla, olfactory bulb, and hypothalamus. Hypothalamic neurons that express NPY also coexpress the leptin receptor and are believed to play a key role in regulating feeding behavior (*20*). In these experiments, we used a bacterial artificial chromosome (BAC) transgenic mouse line that carries a modified 150-kb *Npy* BAC in which the *Cre recombinase* gene was inserted by homologous recombination into the ATG of the first exon of the *Npy* gene (Fig. 2B) (*21*). In the resulting BAC, 30 kb of 5′ upstream sequence and 90 kb of sequences 3′ to the *Npy* gene flank a *Cre*-poly(A$^+$) cassette. To confirm that the recombination event occurred only in NPY-Cre–expressing cells, we constructed a *tk*$^-$ virus conditional only for GFP expression (Fig. 2A). Because

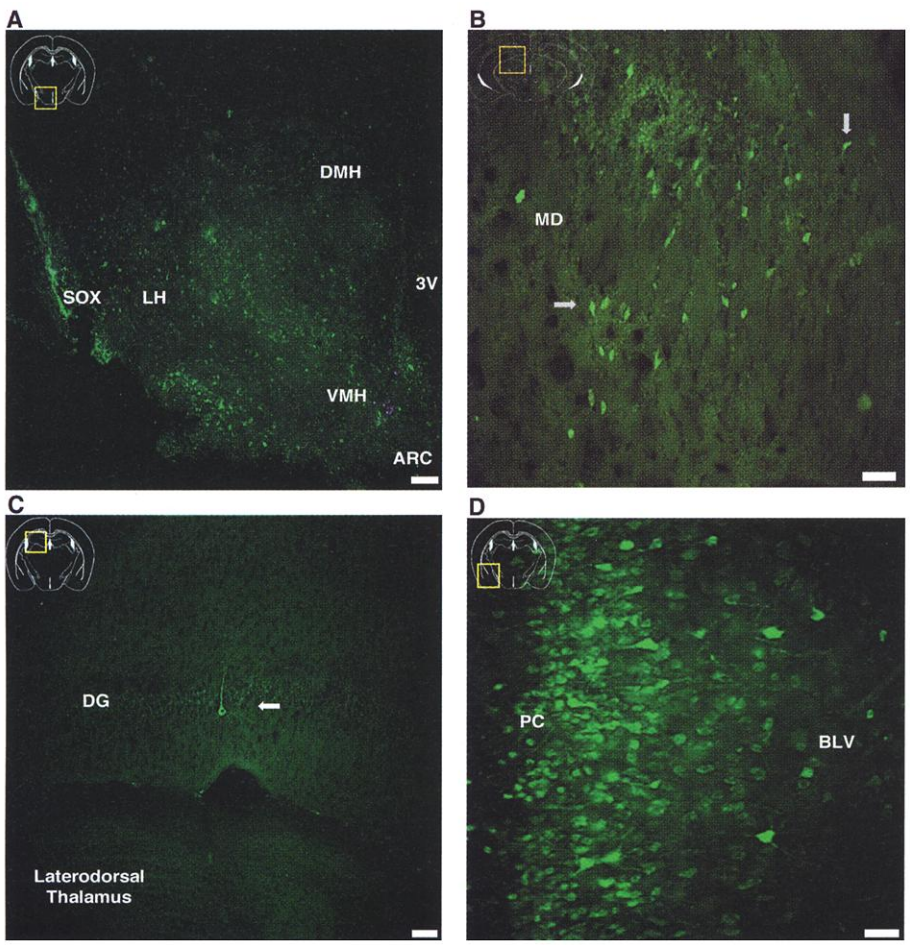

Fig. 3. Ba2001 infection of NPY-Cre mice after injection into the arcuate nucleus. *Npy-Cre* transgenic mice were killed 4 days after injection of 1.1×10^6 PFUs of Ba2001 into the arcuate nucleus. (**A**) Viral spread within the posterior hypothalamus. GFP was expressed in the following hypothalamic structures as indicated: ARC, arcuate nucleus; DMH, dorsomedial nucleus; LH, lateral hypothalamus; VMH, ventromedial hypothalamus; SOX, supraoptic decussation; 3V, third ventricle. Scale bar, 100 μm. (**B**) Viral spread to the medial dorsal thalamus (MD). Arrows indicate locations of GFP fluorescent neurons. Scale bar, 25 μm. (**C**) Viral spread to the dentate gyrus (DG). Scale bar, 25 μm. (**D**) GFP expression in the piriform cortex (PC) and ventral basolateral amygdala (BLV) 5 days postinfection. Scale bar, 25 μm.

this virus is defective for DNA replication, the expression of Tau-GFP should be restricted to those neurons that express NPY (and Cre). After cortical injections of the virus into NPY-Cre mice, large numbers of NPY-expressing cell bodies (scored using a specific antibody against NPY) were observed proximal to the injection site (Fig. 2C, left). GFP fluorescence was evident only in a subset of these neurons (Fig. 2C, middle). Superimposition of the NPY antibody and GFP images revealed yellow and red, but not green, cells (Fig. 2C, right). If GFP expression were independent of Cre, green cells would have been observed. These data confirmed that, in these mice, GFP expression was restricted to Cre- and NPY-expressing neurons.

To map neural inputs to NPY-expressing cells that play a role in regulating feeding behavior, we injected Ba2001 into the arcuate nucleus of the NPY-Cre mice stereotaxically. The arcuate nucleus is the hypothalamic site with the highest level of NPY expression (*22*). Mice were killed at various times after infection, and the pattern of expression of GFP was examined in serial sections of whole brains. At early times, GFP was expressed in several other hypothalamic nuclei, most notably the VMH and LH (Fig. 3A). This result confirms previous evidence that the arcuate nucleus receives inputs from these other hypothalamic nuclei (*23*). Retrograde infection by the virus from the hypothalamus was also observed in the medial dorsal nucleus of the thalamus (MD) (Fig. 3B) and the dentate gyrus (DG) (Fig. 3C). Five days after infection, the infection had spread to the piriform cortex (Pir) and the ventral basolateral amygdala (BLV) (Fig. 3D). The later appearance of fluorescence at these sites suggests that they are most likely second- or higher-order neurons. Table 1 summarizes the times at which each of the sites was first visualized and the intensity of fluorescence. At earlier stages of infection, GFP expression is restricted to hypothalamic nuclei. Four days after infection, labeling is present in other sites including the amygdala, bed of stria terminalis (BST), and Pir.

We also attempted to map the inputs to neurons expressing the leptin receptor (ObRb), which is much less abundant than NPY (Fig. 4A). The large size of the *ObR* gene precluded the use of the BAC transgenic approach, so we introduced an IRES-Cre cassette by homologous recombination immediately 3′ to the *ObRb* stop codon (Fig. 4A). Productive infections were observed after injection of the virus into the hypothalamus but not after injection into the amygdala, Pir, or cerebellum (*17*). This is consistent with the known distribution of ObRb in the brain (*24*).

We next injected Ba2001 and fluorescent beads (to localize the injection site) into the arcuate nucleus of the ObR-Cre mice and prepared brain sections at various times after infection. A summary of the brain regions visualized after infection is shown in Table 1. As in the NPY experiments, the lag time between viral injection and GFP expression by the various neurons was used to tentatively assign a hierarchy among the connections. At 72 hours postinfection, GFP-expressing neurons were observed in the arcuate nucleus rostral to the injection site (Fig. 4B, left). Although labeled neurons were observed in the contralateral arcuate nucleus, a greater number of labeled neurons were found in the side that received the injection. GFP-expressing neurons were also identified in the LH, VMH, and DMH. Five days after infection, labeled neurons were evident in several extrahypothalamic sites including the basolateral amygdala (BLA), Pir, and lateral entorhinal cortex (LEnt) (Fig. 4C, left). Higher magnification of infected neurons in the BLA revealed what may be a synaptic connection

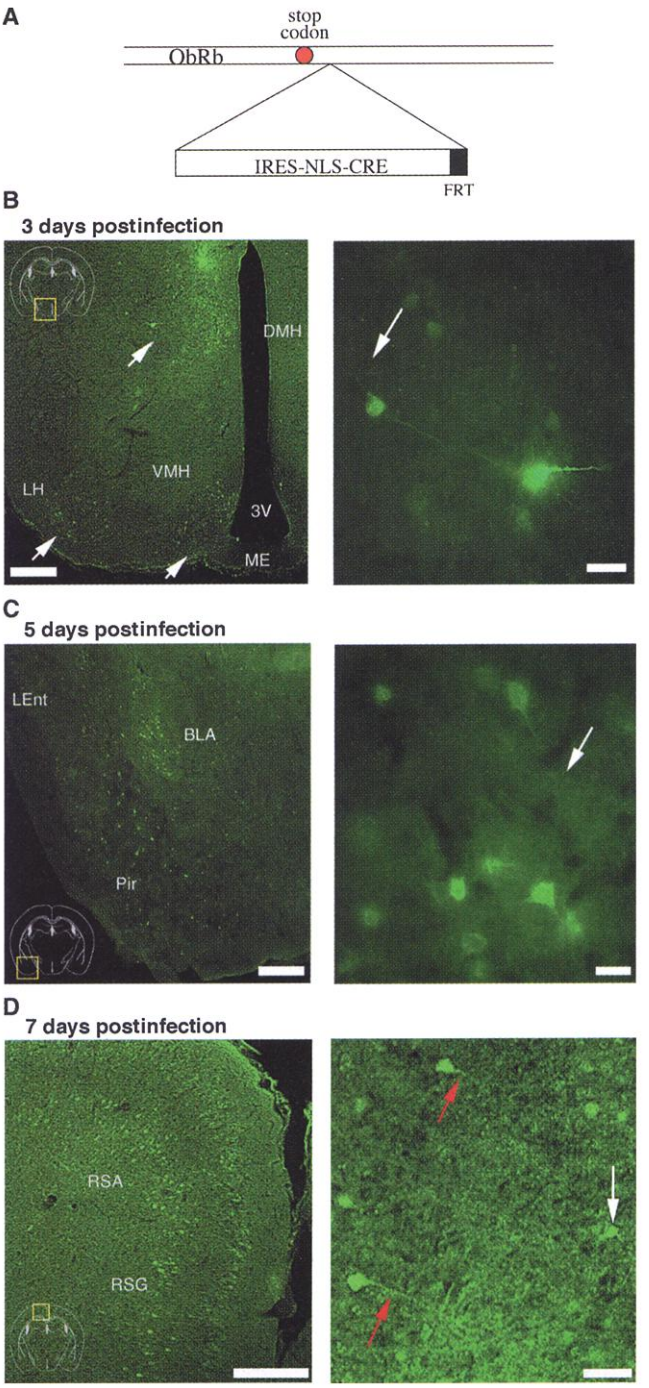

Fig. 4. Ba2001 infection of ObRb-IRES-Cre recombinant mice. A total of 1.3×10^6 PFUs of Ba2001 was injected into the arcuate nucleus of embryonic stem (ES) cell–derived mice that express Cre from an IRES element inserted into the 3′ untranslated region of the *ObR* gene. Animals were killed after infection at the times indicated. Brains were sectioned and GFP expression was visualized by immunofluorescence from antibody against GFP (B to D). Low power (10×) and high power (40×) images are shown on the left and right panels, respectively. (**A**) ObRb-IRES-Cre targeting construct. A cassette containing an IRES-NLS-*Cre* and *neo* gene, flanked by *frt* sites, was inserted immediately 3′ to the stop codon in the last exon of *ObRb*. This cassette was then used for recombination in ES cells, and positive recombinant ES clones were used to generate the *ObRb* "knock-in" mouse. (**B**) Expression of GFP in the hypothalamus 3 days postinfection. At 3 days, GFP was expressed in the arcuate, DMH, LH, and VMH. Higher magnification of the DMH (right panel) revealed a possible connection between two DMH neurons (white arrow). Scale bars: left, 200 μm; right, 25 μm. (**C**) GFP expression in the limbic and cortical brain regions. GFP expression in the BLA, Pir, and LEnt 5 days postinfection (left). Population of GFP-expressing neurons in the BLA (right). Scale bars: left, 200 μm; right, 25 μm. (**D**) GFP expression in the retrosplenial cortex 7 days postinfection. GFP-expressing neurons in the granular retrosplenial and agranular cortex. Right panel illustrates cells with the morphology of pyramidal cells (red arrows) and interneurons (white arrow). Scale bars: left, 200 μm; right, 50 μm.

between neurons, a possibility that can be confirmed using electron microscopy (Fig. 4C, right). Labeled neurons were also observed in the agranular and granular retrosplenial cortex (Fig. 4D). In this region, the morphology of the GFP-expressing cells suggested that both pyramidal neurons (red arrows) and interneurons (white arrow) were infected. Labeled neurons in these brain regions are most likely second-order or higher because they appear only at later stages of infection. Fluorescence was restricted to small, discrete numbers of neurons in each of these nuclei and revealed that the infected cells are not contiguous. These data are consistent with previous results indicating that the virus spreads predominantly in a transneuronal fashion rather than laterally (*25*).

In addition to the sites shown in Fig. 4, labeling was also observed in several other sites, particularly at later times postinfection (Table 1). Five days after infection, labeling was observed in the perirhinal, entorhinal, and somatosensory 2 cortex. At 7 days, GFP-labeled neurons were visible in the somatosensory 1 and retrosplenial cortex, as well as in the CA1 region of the hippocampus and brainstem nuclei. Although neurons that were first observed at 5 days or later are most likely third-order or higher, further analyses will be necessary to determine the precise number of synapses between these sites and the hypothalamus.

Although there was some overlap between the labeled sites observed for the ObRb-Cre and NPY-Cre mice, more brain areas were labeled in the ObRb-Cre mice. This is consistent with the fact that, in the arcuate nucleus, ObRb is coexpressed with NPY, proopiomelanocortin, and possibly other neurotransmitters (*18*). Thus, in the hypothalamus there are several classes of neurons that express ObR, only one of which coexpresses NPY. The GFP-positive sites that are seen only in the ObR-Cre mice may have resulted from projections to infected ObR neurons that do not express NPY.

In summary, we have used a conditional pseudorabies virus to trace the afferent connections of arcuate neurons that express either an abundant transcript, NPY, or a low-abundance transcript, ObRb. In many cases our data are consistent with previous studies in which the connections of unspecified neurons were mapped. In other instances, previously unknown connections have been visualized. For example, projections from the BLA, Pir, and BST to the hypothalamus have been reported using other tracing methods, but the connections from the retrosplenial cortex and LEnt to the hypothalamus have not been detected previously (*26–28*). Although our viral tracing experiments revealed a variety of afferent inputs in both NPY- and ObRb-Cre mice, it is also possible that additional inputs exist that have escaped detection.

Although the kinetics of neuronal labeling can be used to establish a hierarchy of connections, the designation of neurons as first-, second-, third-, and fourth-order, and so on, is not yet confirmed. Further studies including three-dimensional reconstruction of these images should reveal the precise nature of the connections to the hypothalamus from these brain regions.

These data indicate that hypothalamic neurons that express the leptin receptor receive inputs from a number of CNS centers and are likely to integrate signals from these other sites before in turn transmitting impulses to a set of as yet unidentified, efferent sites. Modifications to this viral tracing system using PRV strains that can be transmitted in the anterograde direction may also make it possible to trace these efferent connections (*29*). This method and modifications to it may prove useful in studies of other complex neural circuits.

Table 1. Summary of Ba2001 infections in NPY-Cre and ObRb-Cre mice. Data from all of the experiments were compiled and the CNS sites that expressed GFP after infections by Ba2001 are shown. Column 1 lists the anatomic sites where GFP expression was observed in the infected NPY-Cre and/or ObRb-Cre mice. Column 2 shows the time postinfection, in days, when GFP labeling was first observed. Columns 3 and 4 show results from Ba2001 infection time course in NPY-Cre transgenic mice. Columns 5 and 6 show results from Ba2001 infection time course in ObRb-IRES-Cre mice. Frequency, the fraction of mice out of the total that expressed GFP at that site. ND, not done. Intensity rating, +++ indicates uniform site labeling intensity among all mice examined; ++, site labeled in all mice with one or more showing decreased intensity; +, site labeled in some but not all mice; −, no labeling observed in any mice.

GFP-labeled sites	Time postinfection	NPY-Cre		ObRb-IRES-Cre	
		Frequency	Intensity	Frequency	Intensity
Arcuate nucleus	1.5 days	2/2	+++	4/4	+++
Ventromedial hypothalamus	3	3/3	+++	5/5	+++
Dorsomedial hypothalamus	3	3/3	++	5/5	+++
Lateral hypothalamus	3	3/3	++	5/5	++
Paraventricular nucleus	3	2/3	+	5/5	++
Suprachiasmatic nucleus	3	0/2	−	3/5	+
Amygdala	4	2/2	+++	4/4	+++
Bed of stria terminalis	4	2/2	+++	4/4	++
Piriform cortex	4	1/2 (5 days)	+	3/4	+
Thalamus	4	1/2	+	0/4	−
Lateral entorhinal cortex	5	ND	−	5/5	++
Perirhinal cortex	5	ND	−	5/5	++
Somatosensory cortex 2	5	ND	−	3/5	+
Mesencephalic trigeminal nucleus	5	ND	−	1/5	+
Somatosensory cortex 1	7	0/2	−	3/3	+++
Retrosplenial cortex	7	0/2	−	3/3	++
CA1/hippocampus	7	1/2 (4 days)	+	1/3	+
Lat. paragigantacellular nucleus	7	0/2	−	1/3	+
Raphe magnus	7	0/2	−	1/3	+

References and Notes

1. J. M. Friedman, J. L. Halaas, *Nature* **395**, 763 (1998).
2. J. L. Halaas *et al.*, *Proc. Natl. Acad. Sci. U.S.A.* **94**, 8878 (1997).
3. J. K. Elmquist *et al.*, *Proc. Natl. Acad. Sci. U.S.A.* **95**, 741 (1998).
4. L. W. Enquist *et al.*, *Adv. Virus. Res.* **51**, 237 (1998).
5. A. D. Loewy, *Neurosci. Biobehav. Rev.* **22**, 679 (1998).
6. J. P. Card *et al.*, *J. Comp. Neurol.* **407**, 438 (1999).
7. A. Standish *et al.*, *J. Neurovirol.* **1**, 359 (1995).
8. S. Heffner, F. Kovacs, B. G. Klupp, T. C. Mettenleiter, *J. Virol.* **67**, 1529 (1993).
9. To construct Ba2000, we inserted a fragment encoding Tau-GFP [I. Rodriguez *et al.*, *Cell* **97**, 199 (1999)] was inserted into Xho I/Xba I sites of pcDNA3. The *Lox*-Stop-*Lox* cassette from pBS302 (Gibco-BRL, Gaithersburg, MD) was generated by polymerase chain reaction (PCR) and inserted into the Kpn I site of the above construct to give the plasmid pLT. The region containing the CMV promoter to the poly(A$^+$) site was then inserted into the Bam HI/Not I sites in the PRV genomic subclone pGS202 to give pG2LT. To construct Ba2001, we ligated an IRES-*tk* fragment into the Xba I site downstream of the Tau-GFP cassette in pG2LT. Cotransfection of BaBlu and transfer vector DNA and blue-white plaque screening was done as previously described [A. Knapp, L. Enquist, *J. Virol.* **71**, 2731 (1997)].
10. M. Lakso *et al.*, *Proc. Natl. Acad. Sci. U.S.A.* **89**, 6232 (1992).
11. Supplementary material is available on *Science* Online at www.sciencemag.org/cgi/content/full/291/5513/2608/DC1
12. Y. Gordon *et al.*, *Arch. Virol.* **76**, 39 (1983).
13. C. Logvinoff, A. L. Epstein, *J. Virol.* **74**, 8402 (2000).
14. The Synapsin1-Cre transgenic mouse (line 671) was created by linking the rat synapsin-1 promoter (4.4-kb Sal I–Xho I fragment of pBL4.3Syn-CAT) [C. Hoesche *et al.*, *J. Biol. Chem.* **268**, 26494 (1993)] containing 100 bases of 5′ untranslated CAT sequence to a modified *Cre recombinase* bearing Kozak translational consensus and nuclear localization signals. The *Syn1-Cre* transgene included 3′ human growth hormone sequences that provide transcriptional termination and polyadenylation signals [T. Hennet *et al.*, *Proc. Natl. Acad. Sci. U.S.A.* **92**, 12070 (1995)]. Transgenic mice were produced by pronuclear injection of C57BL/6 × CBA (F_2) zygotes. The transgene was bred into and maintained in the C57BL/6 background for more than four generations before characterization (Y. Zhu *et al.*, personal communication).
15. A. K. Robbins *et al.*, *J. Virol.* **58**, 339 (1986).
16. After injection of virus into the right side of the brain, we killed the animals 6 days after infection. We then removed the brains, cut sagittally at midline, and

analyzed tissue samples from brain. Brain tissue was minced, transferred to a 1.5-ml microcentrifuge tube, and washed twice with sterile phosphate-buffered saline (PBS). Tissue chunks were resuspended in 1.0 ml Dulbecco's MEM with 2% serum. The tissue was then homogenized and subjected to three freeze-thaw cycles. Particulate matter was pelleted and the supernatant was used for plaque assays.
17. J. DeFalco, unpublished observations.
18. J. C. Erickson, G. Hollopeter, R. D. Palmiter, *Science* **274**, 1704 (1996).
19. H. Higuchi, H. Y. Yang, S. L. Sabol, *J. Biol. Chem.* **263**, 6288 (1988).
20. C. Elias *et al.*, *Neuron* **23**, 775 (1999).
21. BAC clones containing the *Npy* gene were identified by hybridization to a mouse BAC library filter array using a mouse *Npy* cDNA fragment. A pSV1 shuttle vector subclone containing *Npy* exons 1 and 2 was subsequently generated to give pSV1-*Npy*. Using PCR, we mutated the first ATG to ATT and introduced a Pac I site directly 3′ to the mutated ATG. PCR was used to generate an NLS-*Cre*-SV40 poly(A$^+$) which was then inserted into the Pac I site of pSV1-*Npy*. Recombination into the BAC clone was performed as in X. W. Yang *et al.* [*Nature Biotechnol.* **15**, 859 (1997)].
22. D. R. Gehlert *et al.*, *Synapse* **1**, 25 (1987).
23. L. Zaborsky, *Adv. Anat. Embryol. Cell Biol.* **69**, 1 (1982).
24. H. Fei *et al.*, *Prod. Natl. Acad. Sci. U.S.A.* **94**, 7001 (1997).
25. J. P. Card *et al.*, *J. Neurosci.* **10**, 1974 (1990).
26. F. C. Barone *et al.*, *Brain Res. Bull.* **7**, 75 (1981).
27. H. Bester, J. M. Besson, J. F. Bernard, *J. Comp. Neurol.* **383**, 245 (1997).
28. G. D. Petrovich, P. Y. Risold, L. W. Swanson, *J. Comp. Neurol.* **374**, 387 (1996).
29. M. Yang *et al.*, *J. Virol.* **73**, 4350 (1999).
30. Intracerebral virus injections were performed as in J. P. Card *et al.* [*J. Comp. Neurol.* **407**, 438 (1999)] with two exceptions: a 32-gauge cannula was used to minimize tissue trauma and fluorescent microspheres (Molecular Probes, Eugene, OR) were coinjected to mark injection site. Striatal injection coordinates were +0.38 mm bregma, 1.5 mm lateral of sagittal suture, and −3.5 mm dorsal-ventral. For cortex injections, coordinates were −1.2 mm bregma, 3.65 mm lateral and −2.65 dorsal-ventral. Coordinates for arcuate injections were: −1.9 mm bregma, 0.15 mm lateral, and −5.5 mm dorsal-ventral. A total of 100 nl of virus was injected at a rate of 10 nl/min. The needle was removed after 10 min.
31. Animals were killed by pentobarbital overdose and perfused with 4% paraformaldehyde in PBS. Brains were postfixed, equilibrated in PBS + 30% sucrose and sectioned serially on a cryostat. For immunofluorescence, sections were blocked in PBS with 2% goat serum, 3% bovine serum albumin, and 0.1% Triton X-100 and incubated with the respective primary antibody according to the supplier's recommendations. Antibodies against NPY were obtained from Peninsula Labs (San Carlos, CA). Monoclonal antibodies against gC were purchased from Chemicon (Temecula, CA). Sections were then washed and incubated in FITC or TRITC secondary antibody. Primary antibody dilutions used were as follows: against gC, 1:1000; against NPY, 1:10,000; against GFP, 1:350. Sections were examined using a Zeiss Axioplan microscope. Images were collected using a Princeton Graphics digital camera and processed using IPLab Powermicrotome deconvolution software from Scanolytics (Fairfax, VA).
32. We thank H. Westphal for CMV-Cre mice; S. Dymecki for hACTB::FLP mice; A. L. Epstein for TE-Cre cells; M. Kiliman for pBL4.3Syn-CAT; A. Soukas and A. Viale for assistance with animal surgery and sectioning, respectively; P. Mombaerts and the Rockefeller GFT for assistance with ES cell recombination; C. Saper for neuroanatomical advice; M. B. Hatton and N. Heintz for critical reading of this manuscript; S. Korres for assistance in preparing this manuscript. J.M.F. was supported by NIH grant R01DK41096. J.D.M. was supported by a grant from the Institute of Diabetes and Digestive and Kidney Disease, National Institutes of Health (DK48247). L.E. was supported by NIH grant R01133506.

16 October 2000; accepted 21 February 2001

Continuous Fatty Acid Oxidation and Reduced Fat Storage in Mice Lacking Acetyl-CoA Carboxylase 2

Lutfi Abu-Elheiga,[1] Martin M. Matzuk,[2] Khaled A. H. Abo-Hashema,[1] Salih J. Wakil[1]*

Malonyl–coenzyme A (malonyl-CoA), generated by acetyl-CoA carboxylases ACC1 and ACC2, is a key metabolite in the regulation of energy homeostasis. Here, we show that *Acc2*$^{-/-}$ mutant mice have a normal life span, a higher fatty acid oxidation rate, and lower amounts of fat. In comparison to the wild type, Acc2-deficient mice had 10- and 30-fold lower levels of malonyl-CoA in heart and muscle, respectively. The fatty acid oxidation rate in the soleus muscle of the *Acc2*$^{-/-}$ mice was 30% higher than that of wild-type mice and was not affected by addition of insulin; however, addition of insulin to the wild-type muscle reduced fatty acid oxidation by 45%. The mutant mice accumulated 50% less fat in their adipose tissue than did wild-type mice. These results raise the possibility that pharmacological manipulation of ACC2 may lead to loss of body fat in the context of normal caloric intake.

Acetyl–coenzyme A (acetyl-CoA) carboxylase (ACC) catalyzes the synthesis of malonyl-CoA, a metabolite that plays a pivotal role in the synthesis of fatty acids as the donor of "C_2 units" (*1–3*) and in the oxidation of fatty acid as the regulator of the mitochondrial shuttle system (*4, 5*). Hence, ACC links fatty acid and carbohydrate metabolism through the shared intermediate acetyl-CoA, the product of pyruvate dehydrogenase. Deciphering the roles of ACC in energy metabolism in lipogenic tissues (liver and adipose) and nonlipogenic tissues (heart and muscle) has become the focus of many studies (*4–11*). In animals, including humans, there are two isoforms of acetyl-CoA carboxylase, ACC1 [relative molecular mass (M_r) ~ 265,000] and ACC2 (M_r ~ 280,000), which are encoded by separate genes and display distinct tissue distributions (*12–16*). ACC1 is highly expressed in liver and adipose tissue, whereas ACC2 is predominantly expressed in heart and muscle, and to a lesser extent in liver (*3, 13–17*). ACC2 is localized in the mitochondria and ACC1 in the cytosol (*6*).

The carboxylases are highly regulated by diet, hormones, and other physiological factors. Food intake, especially fat-free diets, induces the synthesis of ACCs and increases their activities. Starvation or diabetes mellitus represses the expression of the ACC genes and decreases the activities of the enzymes. Malonyl-CoA, the product of ACC1 and ACC2, is the key metabolic signal for the control of fatty acid oxidation and synthesis in response to dietary changes. Among the critical unanswered questions are whether malonyl-CoA pools exist that differentially control fatty acid oxidation and synthesis, whether these putative pools can be independently manipulated, and if so, what would be the physiological consequences of such manipulation. To examine these issues, we generated ACC2-deficient mice.

A mouse Acc2 genomic clone was isolated using an Acc2 cDNA probe, and a targeting vector was constructed to generate embryonic stem cells with one mutant copy of the *Acc2*^{tm1AE} allele (Fig. 1A). Heterozygotes did not have any obvious abnormalities. Genotype analysis of offspring from heterozygous matings were consistent with Mendelian inheritance [24% *Acc2*$^{-/-}$ (n = 72), 54% *Acc2*$^{+/-}$ (n = 162), and 22% wild type (n = 66); (Fig. 1B)]. Northern blot (Fig. 1C) and Western blot (Fig. 1D) analyses indicated that the *Acc2*^{tm1AE} allele was null. The *Acc2*$^{-/-}$ mutants are fertile and appear to have a normal life span.

Because malonyl-CoA is generated by both ACC1 and ACC2, we investigated whether ACC1 can compensate for the absence of ACC2. ACC activities in wild-type and mutant livers were the same (1.3 and 2.4 nmol/min/mg of protein in the absence and presence of citrate, respectively), suggesting that malonyl-CoA in the mutant liver is pro-

[1]Verna and Marrs McLean Department of Biochemistry and Molecular Biology and [2]Departments of Pathology, Molecular and Cellular Biology, and Molecular and Human Genetics, Baylor College of Medicine, Houston, TX 77030, USA.

*To whom correspondence should be addressed. E-mail: swakil@bcm.tmc.edu